JGR Biogeosciences

RESEARCH ARTICLE
10.1029/2020JG005976

Recovery: Fast and Slow—Vegetation Response During the 2012–2016 California Drought

Xi Yang[1], Xiangtao Xu[2], Atticus Stovall[1,3], Min Chen[4,5], and Jung-Eun Lee[6]

[1]Department of Environmental Sciences, University of Virginia, Charlottesville, VA, USA, [2]Department of Ecology and Evolutionary Biology, Cornell University, Ithaca, NY, USA, [3]Biospheric Sciences Lab, NASA Goddard Space Flight Center, Greenbelt, MD, USA, [4]Joint Global Change Research Institute, Pacific Northwest National Laboratory, College Park, MD, USA, [5]Department of Forest and Wildlife Ecology, University of Wisconsin-Madison, Madison, WI, USA, [6]Department of Earth, Environmental, and Planetary Sciences, Brown University, Providence, RI, USA

Key Points:

- Abrupt and gradual vegetation responses to the California drought were observed
- Vegetation responses were driven by both biotic and abiotic factors
- Thirty-three percent of the natural vegetation in California has recovered to the level of 2010

Correspondence to:
X. Yang,
xiyang@virginia.edu

Citation:
Yang, X., Xu, X., Stovall, A., Chen, M., & Lee, J.-E. (2021). Recovery: Fast and slow—vegetation response during the 2012–2016 California drought. *Journal of Geophysical Research: Biogeosciences*, *126*, e2020JG005976. https://doi.org/10.1029/2020JG005976

Received 19 JUL 2020
Accepted 18 FEB 2021

Abstract The 2012–2016 California Drought severely impacted natural vegetation across a wide range of environmental gradient. Although several studies have reported an increase in plant water stress and mortality, the spatiotemporal variations of ecosystem productivity responses and the associated environmental and biological drivers remain unclear. Here, using Enhanced Vegetation Index from the Moderate resolution imaging spectrometer, we found that 45% of the natural ecosystems showed an abrupt change (breakpoint [BP]) in productivity during 2012–2016. There were three major contrasting temporal patterns of productivity responses: (i) a steady increase under higher temperature followed by a decline due to accumulated moisture depletion (high elevation forest) or temperature decrease (high elevation nonforest), (ii) gradual decline during the drought followed by a rapid recovery within 1 year after drought stress was partially relieved, and (iii) both a gradual decline and an abrupt decline. The magnitude of abrupt changes was negatively correlated ($r = -0.80$, $p < 0.001$) with initial gradual changes. Overall, changes during BP offset, on average, 57% of the preceding gradual responses. The spatial variability in ecosystem response patterns is driven by both environmental and biological factors. Particularly, for forests, positive BP was driven by increasing rainfall and decreasing temperature, while negative BP was mainly driven by the precipitation anomaly. By 2019, 33% of the natural vegetation have recovered to the level of EVI in 2010. Ecosystem responses to multiyear droughts can influence ecosystem dynamics in a complex pattern. Multiple ecohydrological factors should be considered to understand and predict the long-term drought impacts on ecosystems.

Plain Language Summary The 2012–2016 California Drought caused significant damage to natural ecosystems throughout the state, many of which are still struggling to return to their previous state. While there are studies on the causes and impacts of this drought, our work identified strong spatial variability in the direction, magnitude, and timescale of vegetation responses. Depending on vegetation type and local environmental factors, ecosystem productivity can either increase or decrease in the early stage of the drought but more than half of the gradual changes in productivity were offset by abrupt changes in the late stage. These results have significant implications in predicting the response of vegetation to drought.

1. Introduction

Drought is an increasing threat to many terrestrial ecosystems (Allen et al., 2015; McDowell et al., 2018, 2020; Miller et al., 2020; Reichstein et al., 2013; Vicente-Serrano et al., 2013). The Californian Mediterranean and Montane ecosystems are some of the most drought-vulnerable areas in the United States because the combination of declining precipitation and increasing temperature with global warming lead to earlier snowmelt and reduced water availability during the summer (Scheff & Frierson, 2012). The 2012–2016 California drought is considered as one of the most severe droughts in the last 1,200 years (Griffin & Anchukaitis, 2014), which has significantly decreased the groundwater level (Famiglietti, 2014), degraded forests (Asner et al., 2016; Stovall et al., 2019), and worsened local air quality (Demetillo et al., 2019). This "exceptional" drought provides a unique natural experiment to observe ecosystem resilience and recovery under unusually prolonged water stress, which is projected to occur with increasing frequency due to anthropogenic changes in atmospheric CO_2 (Diffenbaugh et al., 2015).

Several recent studies have focused on the patterns and drivers of vegetation canopy water loss (Asner et al., 2016) and tree mortality (Goulden & Bales, 2019; Paz-Kagan et al., 2017; Rao et al., 2019; Stovall et al., 2019, 2020) during the 2012–2016 California drought. However, the response of ecosystem productivity, a critical process of the carbon cycle, to the multiyear drought across a large environmental gradient and a wide range of vegetation types is relatively unexplored, particularly during the recovery phase. During meteorological drought, reduction of precipitation and the accompanying heatwave can reduce ecosystem productivity in moisture-limited ecosystems but, potentially, increase ecosystem productivity in energy-limited alpine ecosystems (e.g., the 2003 Europe heatwave over the Alps; Jolly et al., 2005). Accordingly, when the drought conditions terminate, ecosystem productivity can either increase due to the release of moisture limitation or decrease due to a reduction in temperature (Berry & Bjorkman, 1980; Huang et al., 2019). These divergent responses result from complex interactions of different processes including enzymatic activity, stomatal closure, phenology, and vegetation demographics, which operate at different spatial and temporal scales (Anderegg et al., 2015; Brodrick & Asner, 2017; Kannenberg et al., 2019; McDowell et al., 2008; Sperry et al., 2017; Wolf et al., 2016). Characterizing the magnitude, time-scale, and environmental drivers of these opposing effects can help to reveal the integrated mechanisms of ecosystem drought responses.

Aside from local resource conditions, the direction and time-scale of drought responses can also depend on vegetation type. At the coarsest level, trees and grasses display distinctive hydraulic traits, water-use strategies, drought resistance/recovery abilities, and the associated metabolic costs to build new tissues (Baldocchi et al., 2004; Scholes & Archer, 1997; Xu et al., 2015). With generally deeper roots and hydraulically resistant stems, trees are more drought-resistant compared to grasses but can cavitate and require a longer time to recover when crossing mortality thresholds in carbon starvation and hydraulic failure (Adams et al., 2017; McDowell et al., 2008), or the associated biotic stress such as insect attack (Fettig et al., 2019). On the other hand, recent studies have shown that mature trees can be quite resistant to loss of conductivity (Dietrich et al., 2018; Körner, 2019). Therefore, ecosystems dominated by trees should show relatively gradual changes in productivity, whereas the grass-dominated ecosystem should generally have more acute responses.

Using the 2012–2016 California drought as an example, we seek to answer the following questions: (1) What is the magnitude and directionality of ecosystem productivity responses to drought, and are there identifiable abrupt changes in productivity, or alternatively, vegetation responses are gradual and slow as usually being characterized with one single trend? (2) Do tree-dominated and grass-dominated vegetation types show different responses? (3) Have the ecosystems fully recovered from the drought? As Schwalm et al. (2017) have shown, most of the ecosystems recover from a drought within 24 months. In the case of megadroughts, it remains unclear over what timeframe ecosystems recover. (4) What are the environmental and biological factors that explain the spatial variability of ecological drought impacts and recovery?

We combine long-term satellite observations of canopy greenness (as a proxy for vegetation leaf area and chlorophyll content) and geospatial products of environmental variables to address these questions. We reveal abrupt and gradual drought responses using the Breaks for Additive Season and Trend (BFAST) method to analyze the Enhanced Vegetation Index (EVI) from the MODerate resolution Imaging Spectrometer (MODIS) time-series during 2010–2019 (Figure 1, see Section 2 for details). Here, we define abrupt response in terms of statistically significant changes in EVI trend within a year, while gradual responses are changes that can be characterized with a linear regression during this period.

2. Materials and Methods

2.1. MODIS Data

Canopy greenness, as a proxy for vegetation productivity over the drought period, was estimated from the EVI data are from the MODIS 16-day level-3 products with 500 m spatial resolution (MOD13A1) (Huete et al., 2002). EVI is influenced by the total leaf amount and the chlorophyll concentration in the leaves (Huete et al., 2002). Only the EVI data points with the highest quality (QA reliability flag equals to 0 and 1) were used. We used MODIS annual land cover (LC) types (MOD12Q1), based on the International Geosphere-Biosphere Program (IGBP) classification, to identify main LC types in this region, including evergreen needleleaf, shrub and savanna, and grassland. Needleleaf forest and woody savannah are grouped in "Forest," as the definition of woody savannah from IGBP is "Tree cover 30%–60% with mean canopy height

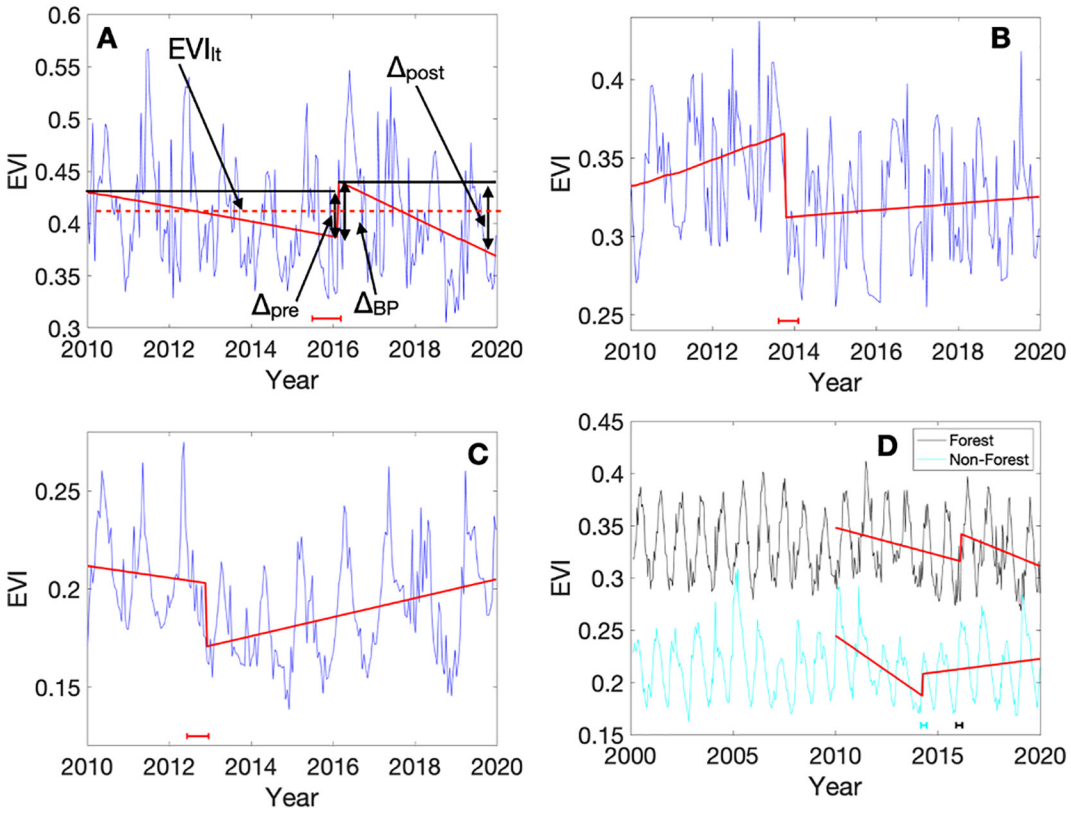

Figure 1. Temporal patterns of ecosystem productivity during the 2012–2016 California drought and the Breaks for Additive Season and Trend (BFAST) terminology in our analyses. We identified three major types of drought responses for vegetations in California: (a) An example of a gradual decline in the Enhanced Vegetation Index (EVI) followed by instantaneous recovery (in terms of a few months to a year) at the BP. We estimated, for each pixel, the long-term mean EVI (EVI_{lt}), the changes before BP (Δpre, %), during BP (ΔBP, %), and after BP (Δpost, %). The uncertainty in the timing of BP is denoted with the red whiskers. (b) A gradual increase in EVI before the BP where there is a precipitous decline of EVI. (c) An example of a decline in EVI before and during BP. (d) Mean time-series of EVI for forest types (forest, and woody savanna as defined by MODIS LC product based on the IGBP classification) and nonforest types (shrub and grass) from 2000 to 2019. We used the full time-series here to show the scale of change during the drought. Red lines are BFAST trend fits, and the uncertainties in the timing of the BPs detected are denoted with whiskers near the *x*-axis.

larger than 2 m." Grassland and savannah are grouped into "non-forest" types. Pixels with LC type changes during this period, particularly from evergreen forests to non-forest types, were excluded. Agriculture and urban pixels were excluded from the analysis. We used MODIS fire product (MCD64A1) to exclude any pixels that had a fire during the 2000–2018 period to avoid false identification of breakpoints (BPs) due to drought. Pixels with a fire history were excluded in this analysis. We also have excluded pixels with mean annual EVI during 2000–2010 <0.15 to exclude areas with minimal vegetation cover. The noisy time-series from these areas have a negative impact on the quality of trend and change detection.

2.2. Breaks for Additive Season and Trend

BFAST is a method to quantify the trend and BPs of time-series, which often have a periodic pattern (Verbesselt et al., 2010). A time-series is decomposed into a trend, a seasonal, and a residual component. BFAST finds whether a significant change of trend exists and when the change is. We used BFAST to quantify the timing of the significant change, which we termed the "breakpoint," the relative magnitude of change in EVI during the BP (calculated as the ratio between the change of EVI and the mean predrought EVI during 2000–2010), and the slope of the trend before and after the BP (Figure 1). There are a few other methods that provides estimates of the timing of BP from remote sensing timer-series, including the Bayesian Estimator of Abrupt change, Seasonal change, and Trend (BEAST; Zhao et al., 2019), a method based on

the ordinary-least squares moving sum test (Forkel et al., 2013), and the R-package "segmented" based on piece-wise regression models (Muggeo & Others, 2008).

The BFAST algorithm also produces the uncertainty in the timing of BP. When there was no statistically significant BP identified, we calculated the slope of the trend component to estimate the total relative change during this period. It is important to note that the number of data points (211) is much larger than the number of variables in the fitted models (6, see Verbesselt et al., 2010), and thus BFAST is unlikely to be overfitted (Verbesselt et al., 2010).

We used the change since 2010 before BP (Δ_{pre}) relative to the long-term EVI (EVI_{lt}) from 2000 to 2010 ($\delta_{pre} = \Delta_{pre}/EVI_{lt}$, %) to assess the gradual response to drought; The relative magnitude of EVI change at BP (Δ_{BP}) to the long-term mean of EVI ($\delta_{BP} = \Delta_{BP}/EVI_{lt}$, %) was used to estimate the short-term response to drought; and the EVI change after BP ($\delta_{post} = \Delta_{post}/EVI_{lt}$, %) relative to the long-term mean EVI (δ_{post}) to estimate the gradual change post BP (Figure 1). EVI_{lt} is the indicator of the average green leaf area when it is under normal climate conditions.

To obtain biologically meaningful BPs that are related to the drought, we conducted the following steps: (1) excluded pixels with uncertainty in the timing of BP larger than 1 year. The excluded pixels may have highly uncertain BP detected. These pixels were then put into the category with no BP, and the relative change to long-term mean during this period was calculated; (2) We also limited the number of BPs to be no more than two and excluded the pixels where the confidence interval range of the BP timing is over 1 year. The rationale is that given the nature and timing of the disturbance, it is unlikely to have more than two BPs in a 10-year period; (3) We excluded pixels with recent fire events and changes of LC types during this period (e.g., forest to cropland).

2.3. Environmental Determinants of Spatial Variations in BFAST Results

To understand the environmental drivers of BFAST results, we used Random Forest Regression (Python scikit-learn 0.19.1 RandomForestRegressor) to investigate the environmental and biological determinants of the ecosystem changes before the breakpoint (δ_{pre}), during the breakpoint (δ_{BP}), and after the breakpoint (δ_{post}). We used 200 trees for each regression. We calculated the partial dependence plots to show the effects of each independent variable on ecosystem changes. Note that all of the independent variables were resampled to the resolution of 500 m.

We used the following datasets for the environmental variables and their derivatives such as the mean values before drought (2000–2010) or slopes of changes during the drought. The details of the variables included in each random forest model are listed in the results section.

2.3.1. Parameter-Elevation Relationships on Independent Slopes Model

Monthly precipitation (PPT), mean temperature (T), and VPD (calculated as the mean of the maximum monthly VPD and minimum monthly VPD) from the parameter-elevation relationships on independent slopes model (PRISM) project are used (Daly and Taylor, 1997). The data range is from 1981 to 2018. The spatial resolution is 30 arcsec. We resampled the data by resampling the PRISM datasets to the MODIS grid. We calculated the monthly anomaly of PPT, T, and VPD relative to the monthly mean and SD from 2000 to 2010. Here, we used the mean PPT, T, and VPD during 1980–2010. We calculated the anomalies of PPT, T, and VPD before, during, and after a BP.

2.3.2. Cumulative Water Deficit

We calculated monthly water deficit as the difference between PPT and actual evapotranspiration (AET), from the California Basin Characterization Model (Flint et al., 2013). We then calculated the 24-month cumulative water deficit (CWD) before the month of the BP identified in BFAST. The model outputs are from October 2010 to September 2016.

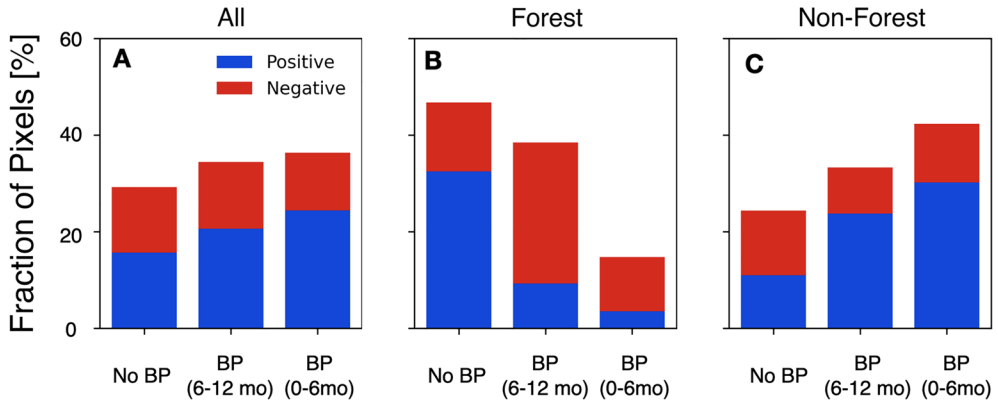

Figure 2. (a) Fractions of pixels with or without BP partitioned by the sign of the change during BP. (b) Same as A, for forests; (c) Same as A, for nonforests. Under the "No BP" category, colors indicate the trend of EVI time-series.

2.3.3. Water Table Depth

Water table depth (WTD) (m) data is the model simulation result constrained by over 1.6 million well and publication records from Fan et al. (2013). WTD values indicate water table depth below land surface. The native resolution of the WTD product is 0.0083°, which is roughly ~1 km in California ~40° latitude).

2.3.4. Soil Available Water Storage

Available water storage (AWS) for the top 150 cm of the soil was calculated as the difference between soil water content at field capacity and the permanent wilting point adjusted for salinity and fragments. It is part of the 2018 version of the USDA Gridded Soil Survey Geographic (gSSURGO) Database (https://www.nrcs.usda.gov/wps/portal/nrcs/detail/soils/home/?cid=nrcs142p2_053628). The original spatial resolution is 30 m.

2.3.5. Elevation

Digital elevation model data used in this study were from the Shutter Radar Topography Mission (SRTM) collected during 2000. The product has a resolution of 90 m.

3. Results and Discussion

3.1. Spatial Variations of Divergent Drought Responses

Here, we show that the uncertainty of BPs is mostly within a year (Figure 2) despite the MODIS data (every 16 days) allow for detection of submonthly abrupt changes, suggesting that vegetation responses to the drought occurred over a few months to a year, instead of an instantaneous vegetation response within 1 or 2 weeks. From 2010 to 2019, 45% of the natural ecosystems had a statistically significant change point detected (Figure 2). Among those areas with BPs, the uncertainties—as estimated by BFAST—in the timing of BP varies (Figure 2): 41% are below 6 months, 49% are between 6 and 12 months. The significant changes in the trend and/or magnitude of EVI during BPs could be caused by beetle attack or drought, which are highly interactive factors that drive the vegetation responses of some evergreen forests (Gaylord et al., 2013; Stovall et al., 2020).

Interestingly, δ_{BP} and δ_{pre} have a strong negative correlation across California ($r = -0.80$, Figure 3), implying that the timing and timescales of drought response vary, probably depending on the characteristics of the ecosystems. The slope of the linear regression between δ_{BP} and δ_{pre} is −0.6, indicating that 60% of the initial gradual changes in productivity, negative or positive, were offset at the BP. Given that almost the entirety of California has experienced equally strong drought conditions (Williams et al., 2015), these patterns suggest that California ecosystems have a wide range of drought resistance and resilience (Malone et al., 2016). Larger initial decreases in productivity mean a higher recovery potential when the environmental stress is relieved. The temporary recovery, despite being induced by short-term changes in climatic conditions

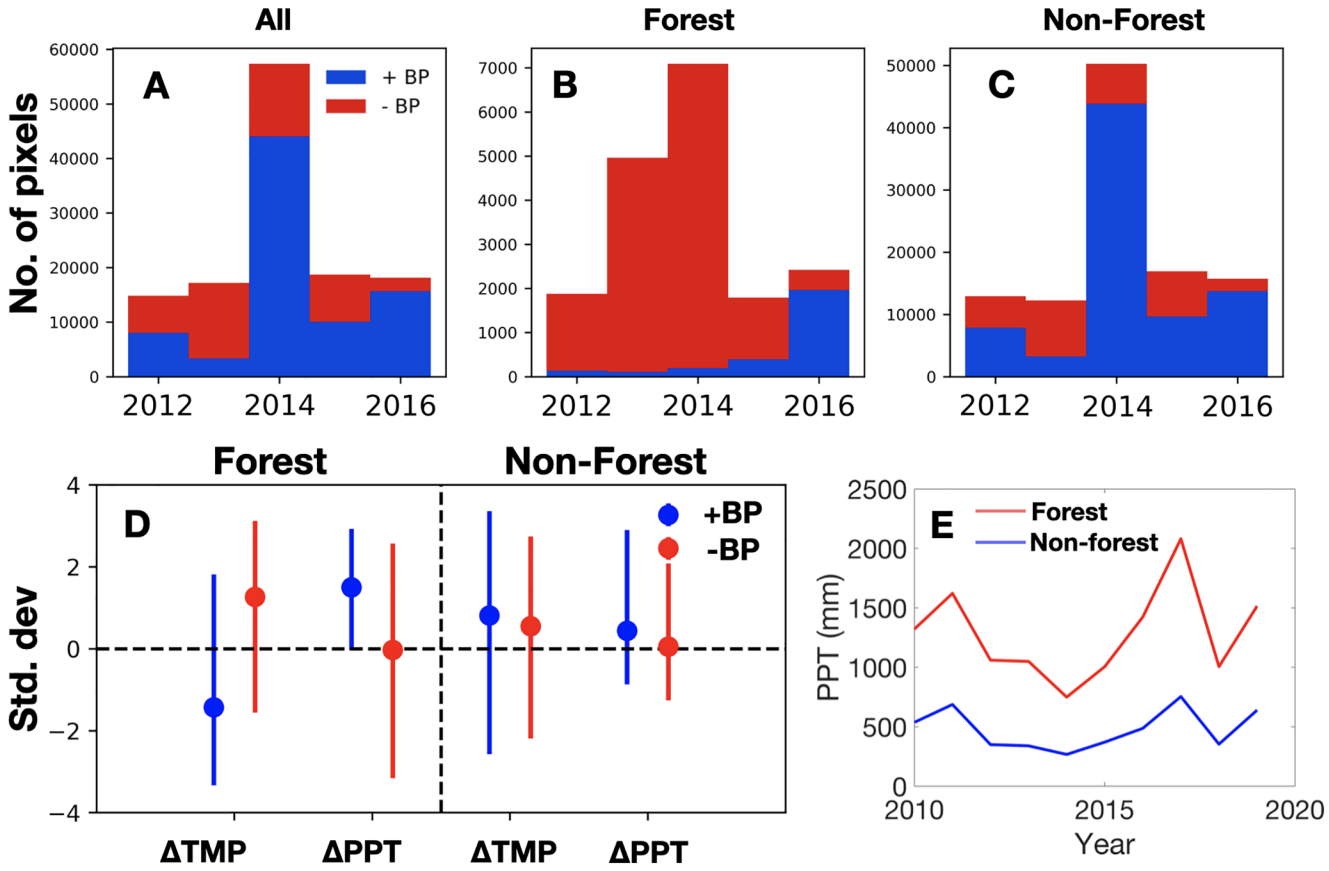

Figure 3. (a) Timing of BP and the sign of BP. (b) Same as D, for forests; (c) Same as D, for nonforests; (d) Anomalies of temperature and precipitation during the BP for forest and nonforest types. Positive BP for forests is associated with lower temperature and positive precipitation. Positive BP for nonforest types is associated with positive temperature and precipitation. (e) Annual precipitation (mm) averaged across all the forest pixels (red) and nonforest pixels (blue).

(Figure 3d), was highly dependent on the preexisting biological responses (δ_{pre}), especially during prolonged droughts like the 2012–2016 California drought.

A majority of the detected BPs have positive signs (58%), implying BP happened during the recovery phase for those regions. This type of recovery could be a transient one following the temporary release of water stress, as we will show later. The likelihood of significant abrupt responses also differs among LC types. Forty-six percent nonforest pixels had BPs between 0 to 6 months, whereas only 24% forest pixels fell in the same category (Figures 2b and 2c). Among the forests, the proportions of positive and negative BPs are 27% and 73%, respectively. A majority of the negative BPs (56%) occurred early during the drought around 2012–2014 (Figure 3a). Among the nonforests, the proportions of positive and negative BPs are 75% and 25%, respectively. For pixels without a BP, more than half of them (56%) have a negative trend during this period, while 44% of them showed a positive trend during this period ($p < 0.001$). Together, the results suggest nonforest types could recover from the drought in a relatively fast and abrupt manner, likely because grasses that dominate these nonforest pixels do not need to invest on stem growth and can regrow quickly once moisture stress is relieved. The pixels with BP uncertainties larger than a year has been treated as pixels without a BP. The EVI time-series of these pixels were only fitted with a linear regression.

The timing of BP varies spatially, but most of the BPs occurred during 2012–2016, with a peak in 2014 (Figure 3b). For forests, negative BPs occurred early in the drought period (2012–2013), while positive BPs were throughout 2015–2016. For nonforests, positive BPs are between 2014 and 2016, and negative BPs are evenly distributed from 2012 to 2015. Even though the drought was at its peak in 2014, precipitation started to recover from then on, likely driving the positive BP of nonforests, which respond faster to precipitation (Figure 3e).

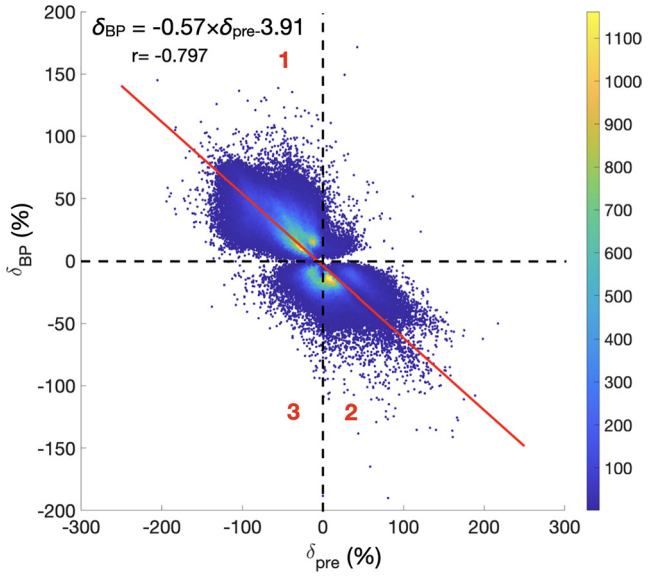

Figure 4. (a) The relationship between changes in EVI before BP (δ_{pre}) and during BP (δ_{BP}). We estimated the changes relative to the long-term mean EVI (2000–2010, EVI_{lt}) before BP (δ_{pre},%), during BP (δ_{BP},%), and after BP (δ_{post},%). Colors of the dots indicate point density. The graph has been divided into three areas corresponding to the text. See text for more details.

The mean EVI time-series of forest and nonforest both showed a BP during the drought that is similar to the first category as described in the next paragraph (Figure 1d). BPs occurred later (2016) in forests, compared to nonforest (2014; Figure 1d). As expected, and suggested by the BFAST results, a large fraction of California's natural ecosystem experienced a loss of productivity during the drought. However, the results also showed that the temporal patterns of drought response and the recovery after the drought cannot be simply characterized by a linear trend throughout the drought period. Post drought responses occurred in either a gradual and fast way, and in either positive or negative directions.

Across the study period, spatiotemporal patterns in California's ecosystem productivity could be grouped into three distinct categories (Figure 4, and see Figure 1 for the corresponding examples): (1) a slow decrease followed by a fast rebound; (2) a slow increase in EVI followed by an abrupt decline; (3) a gradual and a fast decrease often followed by a rebound. Of areas with BPs, 63% of the natural ecosystems had a gradual decrease of EVI, followed by a rebound (Figure 1a, and area 1 in Figure 4); 21% showed a gradual increase in productivity in the early stage of the drought, terminated by a short-term decrease (Figure 1b, and area 2 in Figure 4); 15% had a gradual and an abrupt decrease often followed by a rebound (Figure 1c, and area 3 in Figure 4).

There are clear spatial variations of vegetation response before BP (δ_{pre}, Figure 5c) and during BP (δ_{BP}, Figure 5d). Areas that had reductions in productivity before BP (δ_{pre}) formed a "ring-of-fire" around the Central Valley and can also be found in the southwestern part of the state. Notably, southwestern California showed the most severe drought response and the decline of EVI, as indicated by δ_{pre}, could be as high as the long-term EVI of this region (close to −100% of δ_{pre}, which was calculated as Δ_{pre}/EVI_{lt}).

On the contrary, the forests at a higher elevation (e.g., near the Eldorado National Forest) had a positive δ_{pre} and thus an increasing EVI in the first few years of drought until 2013–2014 (Figures 3b and 5c). This relationship is likely due to larger increases in ecosystem productivity occurring during favorable conditions in a high elevation where the temperature could be the limiting factor at an early drought stage (Jolly et al., 2005). These increases in productivity may have led to over-investment of photosynthetic tissues, an increasing photosynthetic rate and canopy transpiration, further draw-down of local water resources, and ultimately more abrupt decreases when the drought became a prolonged one (Goulden & Bales, 2019; Trugman et al., 2018). The map of change during BP (δ_{BP}) almost mirrored that of δ_{pre} but with an inverse pattern: areas experiencing declines before the BP showed the strongest recovery of EVI (δ_{post} increased up to ~50%), while the western part of the state and areas around the Central Valley had a decline in EVI during the BP. This pattern can also be observed in Figure 4a: pixels in area 1 and 2 had opposite signs of δ_{pre} and δ_{BP}. A few areas, including the northwestern part of the Central Valley, had both negative δ_{pre} and δ_{BP}. After BP, 48% of all the pixels showed a positive recovery (δ_{post}) while 52% showed a negative δ_{post}. There was no clear relationship between δ_{post} and δ_{BP}, indicating that the observed relationship between δ_{pre} and δ_{BP} is not an artifact of the BFAST algorithm.

A significant portion of California's natural ecosystems had not fully recovered from the drought even after 24–36 months of the end of the drought period. By the end of 2019, 33% of the natural vegetation (~7.9 million ha) in California had recovered—as defined by a higher EVI compared to the EVI at the beginning of the drought (i.e., $\delta_{total} > 0$, $\delta_{total} = \delta_{pre}+\delta_{BP}+\delta_{post}$). Sixty-seven percent of areas still have lower EVI compared with that of 2010. We also found that 89% have reached 80% of the predrought vegetation productivity (i.e., most of the pixels with negative δ_{total} had reached at least 80% of the EVI at 2010). Breaking down into forested and nonforested categories, 47% of the forests have fully recovered. Similarly, 21% of nonforests have recovered.

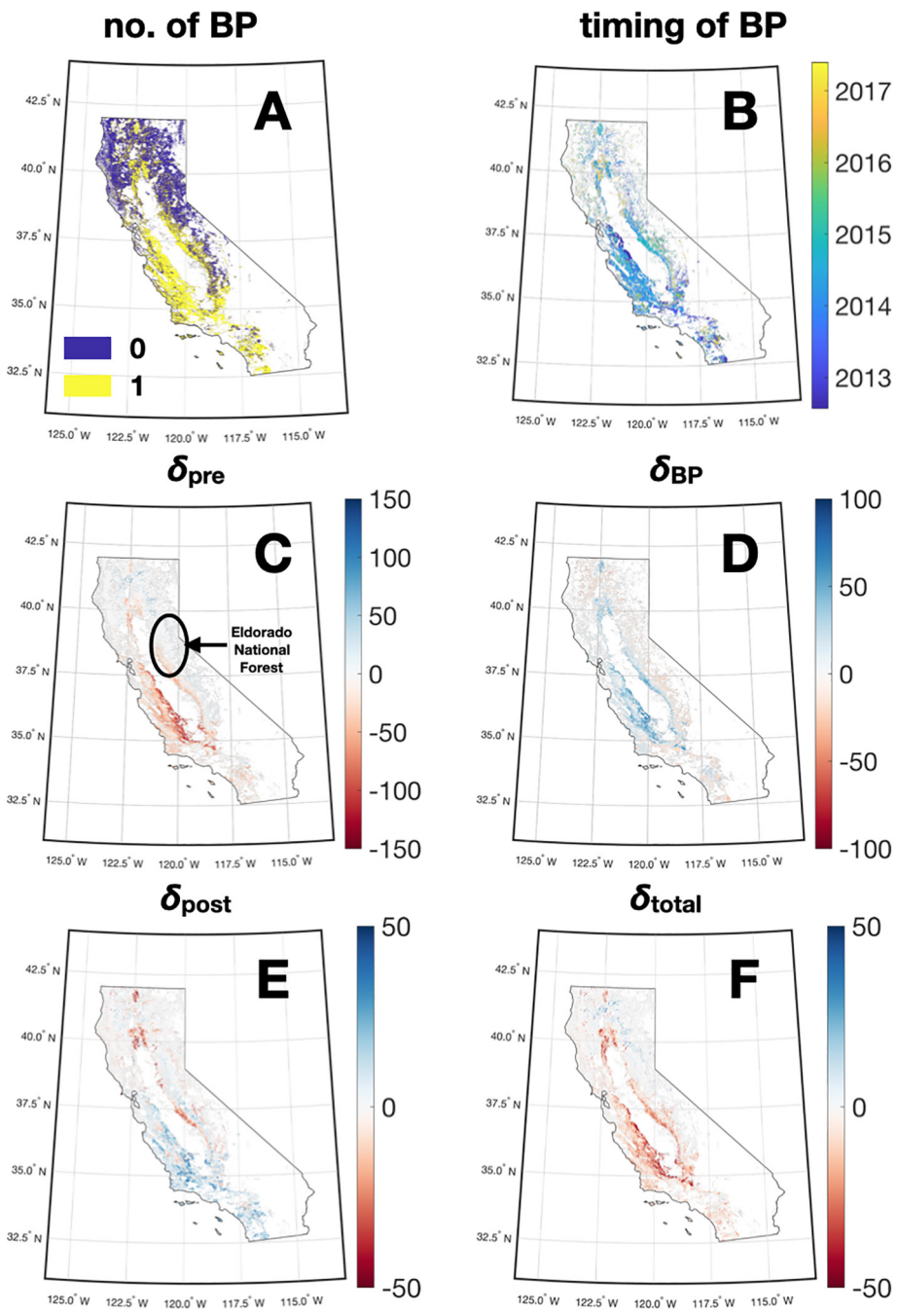

Figure 5. Spatial patterns of vegetation productivity changes in California during 2010–2019 decomposed using BFAST. (a) Number of BPs detected by the BFAST algorithm. One means one BP, whereas zero means no significant BP is detected; (b) The timing of the BP; (c–f) Relative changes compared with long-term (2000–2010) mean EVI at each pixel (EVI_{lt}); (c) Changes before BP (δ_{pre}, %); (d) Changes during BP(δ_{BP}, %); (e) Changes after BP(δ_{post},%); (f) Total change during 2010–2018 relative to the long-term mean ($\delta_{total} = \delta_{pre} + \delta_{BP} + \delta_{post}$,%).

Overall, we showed that the ecosystem response to this megadrought was nonlinear, and the recovery could be characterized by a combination of slow and/or fast responses. Vegetation recovery is a complex process that occurs at various speeds that one single metric (e.g., recovery time) might fail to capture (Schwalm et al., 2017). Nonforest types (grass and shrub) usually had a fast response to changing water availability (increasing or decreasing), whereas forest types were more conservative. Below, we analyze what drivers may have contributed to the fast and slow responses.

Table 1
Key Variables That Contributes to the Spatial Variations of δ_{pre}, δ_{BP}, and δ_{post}

	δ_{pre}	δ_{BP}	δ_{post}
Forest	Historical mean temperature (−)	δ_{pre} (−)	Precipitation trend (+)
	Precipitation anomaly (−)	precipitation anomaly (+)	Altitude (−)
	Historical mean precipitation (−)	Altitude (+)	Temperature trend (−)
	Temperature anomaly (−)		
	VPD anomaly (−)		
Non-forest	Historical mean temperature (−)	δ_{pre} (−)	Historical mean precipitation (−)
	Historical mean precipitation (+)	precipitation anomaly (−)	Temperature trend (+)
	Precipitation anomaly (−)	Altitude (+)	Historical mean temp (−)
	Temperature anomaly (−)	Historical mean precipitation (+)	VPD trend (−)

Forest and nonforest are colored in the same way in the random forest results figures (Figures 6–8). Biotic factors are marked in light green while abiotic factors are marked in blue. The sign after each variable indicates the relationship between the variable and the spatial variations of δ_{pre}, δ_{BP}, and δ_{post}. Only factors with a relative importance value larger than 0.05 are included.

*Note that whenever anomaly is mentioned, it refers to the anomaly of the corresponding period of time, that is, pre BP, during BP, or post BP. Historical mean precipitation is monthly average of a year (so annual mean is 12 times this value).

3.2. Drivers of Vegetation Responses

We used random forest to analyze the potential drivers of the spatial variations in δ_{pre}, δ_{BP}, and δ_{post}. In particular, we were interested in whether the spatial pattern was driven by the variations in the average environment ("climate"), the different degrees of drought stress ("weather"), or any biological variables. We found that both environmental drivers (precipitation and temperature) and the vegetation status before the drought (e.g., EVI_{lt}) drive the response. Key variables that contribute to the spatial variations of δ_{pre}, δ_{BP}, and δ_{post} are summarized in Table 1. Random Forest models explained 80%–90% of the spatial variability of changes in EVI before, during, and after BP.

Forest and nonforest responses before the BP (δ_{pre}) can be well captured by a combination of temperature, precipitation, and VPD during and before the drought (forest, cross-validation $r^2 = 0.84$; nonforest: cross-validation $r^2 = 0.91$, Figure 6). The most important variable that explains the spatial variation of δ_{pre} for forests is the long-term mean annual temperature (TMP_{AVG}), followed by precipitation anomaly before drought (PPT_{pre}), long-term mean annual precipitation (PPT_{AVG}), VPD anomaly before BP (TMP_{pre}), and temperature anomaly before BP (TMP_{pre}). Higher temperature anomaly leads to a more negative response in EVI. This finding is consistent with other work showing that heat stress could be one of the major tree mortality drivers during drought (Stovall et al., 2019). High temperature is oftentimes associated with high vapor pressure deficit, which exacerbates drought stress (Grossiord et al., 2020). Forests with a higher long-term mean annual temperature (TMP_{AVG}) generally had a smaller decrease in EVI, while we did not find a strong relationship between the spatial patterns of TMP_{pre} and TMP_{AVG} ($r = -0.03$). This pattern likely implies the local adaptation to a warmer environment by the drought-tolerating species. For nonforest types, the most important variable is the long-term mean annual temperature (TMP_{AVG}), followed by the long-term mean annual precipitation (PPT_{AVG}), precipitation anomaly before BP (PPT_{pre}), and temperature anomaly before BP (TMP_{pre}). Areas with a higher climatically mean annual precipitation and more precipitation before BP suffered less during this period of time. The average water availability, which reflects the average level of limiting resources, was the second most important (PPT_{AVG}, 16%), whereas elevation had very low relative importance (1%, Figure 6c). We did not find that soil variables such as water table depth and soil available water storage played important roles in driving the spatial variability of δ_{pre}, presumably because of the relatively high uncertainty in these datasets and the sweeping nature of the severity of the drought. Notably, nonforest productivity changes are almost always lower than forest productivity changes under given environmental conditions (brown curves are below green curves in Figure 6), supporting our hypothesis that productivity show more initial gradual increases in forest regions because trees are hydraulically more resistant.

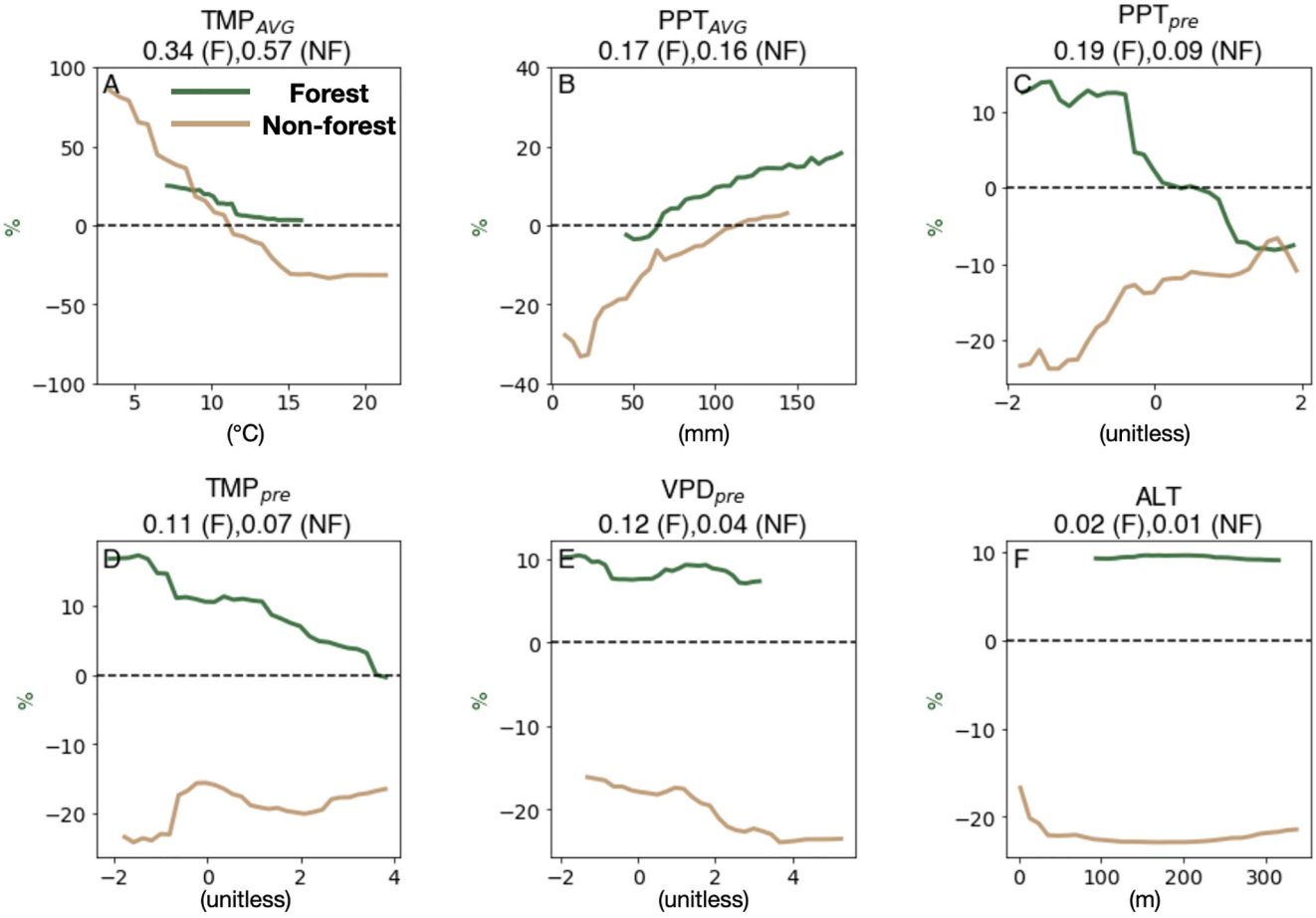

Figure 6. Sensitivity of δ_{pre} to key environmental variables in Random forest analyses. Each panel shows a partial dependence plot with *Y*-axis denoting normalized δ_{pre} and *X*-axis denoting the range of variations of the specific environmental factor as indicated in the panel title. The unit of each driver is under each panel. Each panel title also includes the relative importance of that driver for forest (F) or nonforest (NF). Green lines are for forest, and brown lines are for nonforest. Listed below are the six most important drivers: long-term mean temperature (TMP_{AVG}), long-term mean precipitation (PPT_{AVG}), precipitation anomaly during this period before BP (TMP_{pre}), VPD anomaly during this period before BP (VPD_{pre}), and altitude (ALT).

During the BP, 88% and 93% of the spatial variability of δ_{BP} can be mostly explained by δ_{pre}, and precipitation during this period for forests and nonforests, respectively (Figure 7). The most important factor is δ_{pre}, which is also implicated in Figure 4. The more decline (or increase) before the BP, the more opposite changes during BP, indicating that the ecosystem resilience or memory may have played a role. Besides δ_{pre}, for forests, the most important variable is the precipitation anomaly within one year of the BP (PPT_{BP}), followed by ALT, long-term mean annual temperature (TMP_{AVG}). For nonforests, the second most important variable is PPT_{BP}, followed ALT and PPT_{AVG}. For both forests and non-forests, positive precipitation anomaly seems to be the key to the positive recovery during this period.

After the BP, during the late stage of and after the drought, 80% and 79% of the spatial variability of δ_{post} can be explained by using our Random Forest model (Figure 8). In this analysis, instead of the mean anomaly of precipitation, temperature, and VPD after BP, we used the slope of the precipitation, temperature, and VPD after BP (from BP to 2019) as a group of predictors to the spatial variability of δ_{post}, in combination with historical mean precipitation, temperature, and altitude of each pixel. The main reason for using the slope is that a positive slope could indicate a relief of drought, even when the anomalies of PPT or VPD are still negative. For forests, the most important variable is the slope of precipitation trend (PPT_{slp1}), followed by ALT, the slope of temperature trend (TMP_{slp1}), long-term mean annual precipitation (PPT_{AVG}), the slope of temperature trend (VPD_{slp1}), and long-term mean annual temperature (TMP_{AVG}). Areas with a positive trend of precipitation have more recovery of EVI, which is not surprising. Areas with more historical precipitation

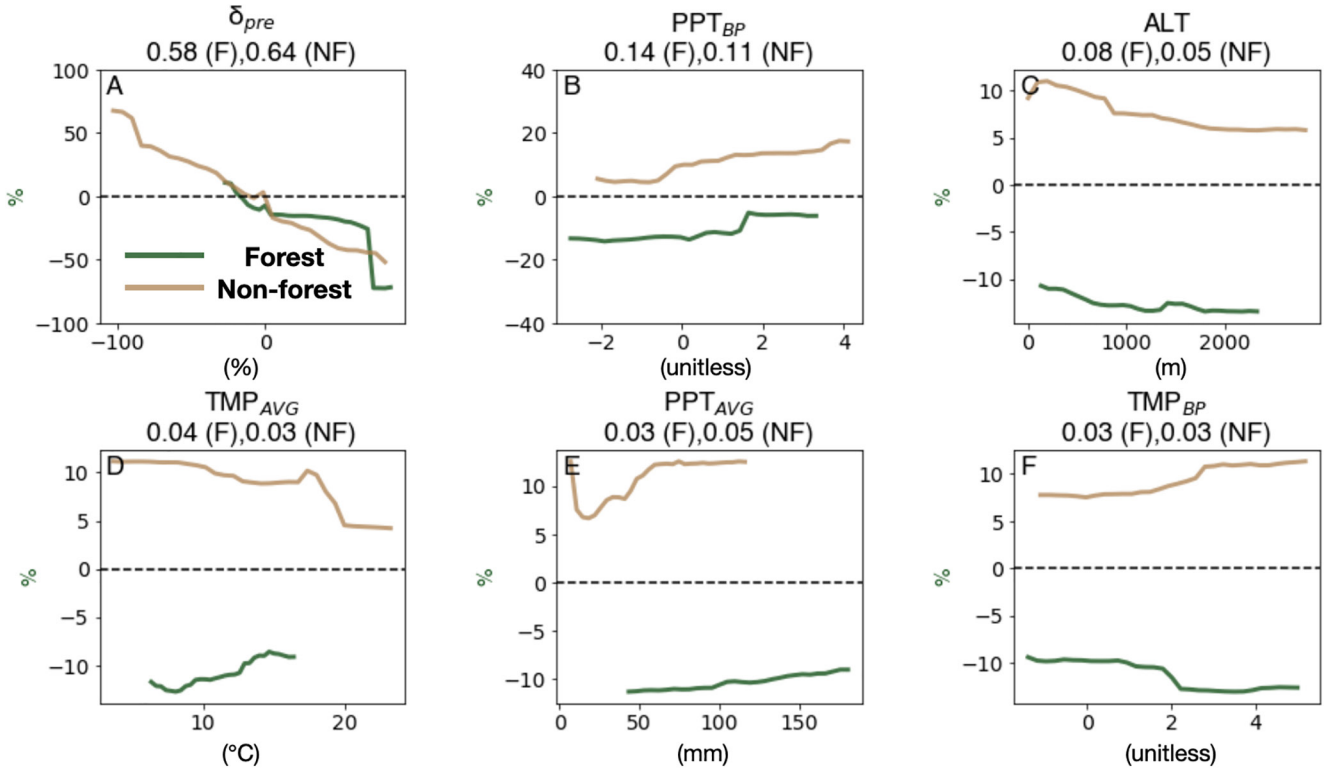

Figure 7. Sensitivity of δ_{BP} to key environmental variables in Random forest analyses. Each panel shows a partial dependence plot with *Y*-axis denoting normalized δ_{BP} and *X*-axis denoting the range of variations of the specific environmental factor as indicated in the panel title. The unit of each driver is under each panel. Each panel indicates one driver and the relative importance of that driver for forest (F) or nonforest (NF). Green lines are for forest, and brown lines are for nonforest. Listed below are the six most important drivers: relative change before BP (δ_{pre}), precipitation anomaly during this period (PPT_{BP}), altitude (ALT), long-term mean temperature during 1980–2010 (TMP_{AVG}), long-term mean precipitation during 1980–2010 (PPT_{AVG}), temperature anomaly during this period (TMP_{BP}).

had a lower recovery rate, likely due to that the vegetation in those areas are less adaptive to drier conditions and thus it takes more water for a full recovery.

Overall, results from random forest analyses suggested the following key findings: (1) the observed changes during the BP and the trends before and after the BP are real instead of artifacts from the BFAST algorithm, because the random forest results by large are in line with ecological understandings; (2) The changes before, during, and after BP are mainly driven by temperature and precipitation anomalies, which can explain a significant portion of the spatial variability of the magnitude and direction of δ_{pre}, δ_{BP}, and δ_{post}. Nonforest types (shrub and grass) seem to be more responsive to instantaneous changes in temperature and precipitation, as supported by a higher R^2 for nonforest types from the random forest analyses. This is not surprising given the relatively lower biomass and shallower root depth of shrub and grass compared with trees in this area. This finding is largely in line with other studies on this topic (e.g., Dong, MacDonald, Willis, et al., 2019; Stovall et al., 2019; Young et al., 2017), in which water deficit is certainly driving the loss of vegetation. Dong, MacDonald, Willis, et al. (2019) showed that there is a difference in drought response between southern and northern California. We have shown in our BFAST results that more areas in the southern California have BPs whereas a significant proportion of northern California does not have a BP. A potential improvement to this study is to examine different nonforest types' response to drought—some shrub species may respond to the drought more like trees than grasses. While MODIS LC types include multiple shrub types (e.g., open shrub or close shrub), they may not closely correspond to the local shrub types that have different ecohydrological traits (e.g., chaparral vs. coastal sage scrub). One study focusing on drought responses of different vegetation types in the Southern California region has shown that temperature is an important driver of vegetation responses to drought, while precipitation is not (Dong, MacDonald, Okin, & Gillespie, 2019). This difference between our study and Dong, MacDonald, Okin, and Gillespie (2019) could

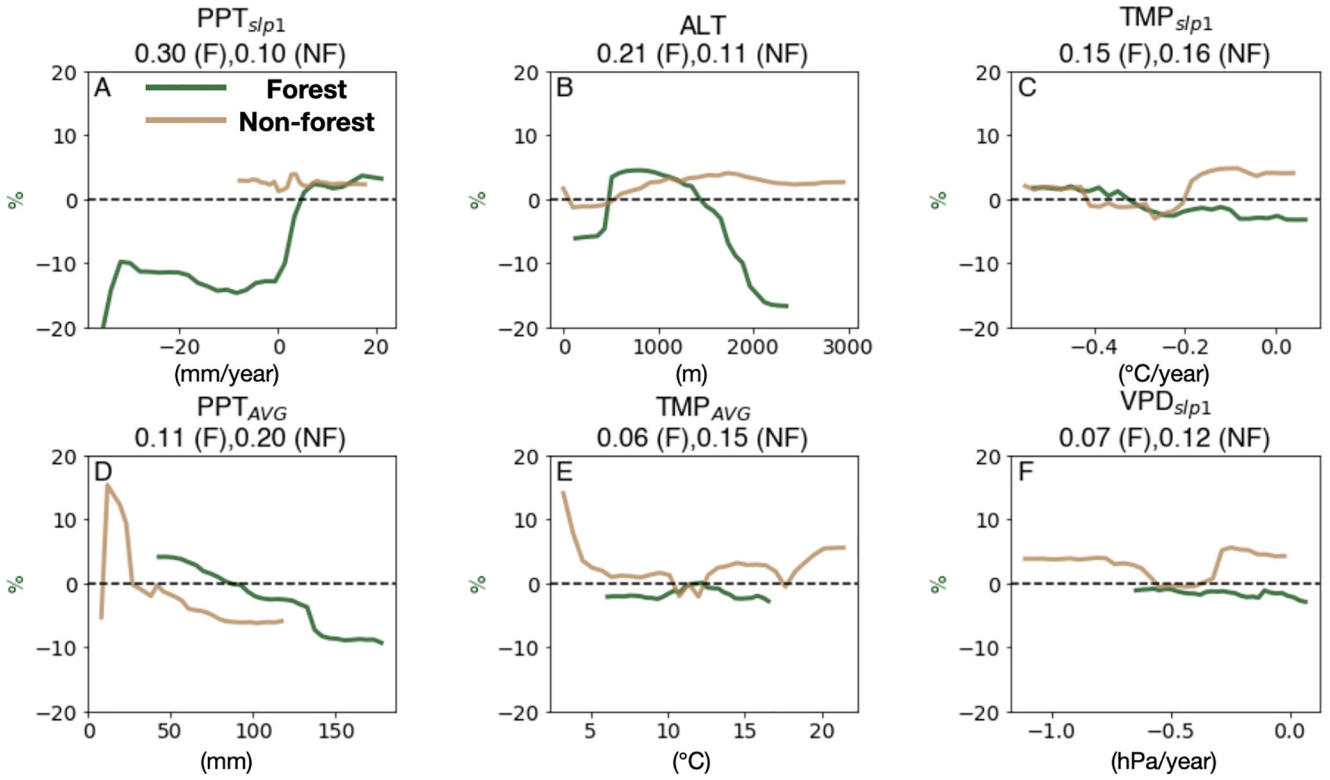

Figure 8. Sensitivity of δ_{post} to key environmental variables in Random forest analyses. Each panel shows a partial dependence plot with *Y*-axis denoting normalized δ_{post} and *X*-axis denoting the range of variations of the specific environmental factor as indicated in the panel title. The unit of each driver is under each panel. Each panel indicates one driver and the relative importance of that driver for forest (F) or nonforest (NF). Green lines are for forest, and brown lines are for nonforest. Listed below are the six most important drivers: the slope of precipitation during this period (VPD_{slp1}), altitude (ALT), the slope of temperature during this period (TMP_{slp1}), long-term mean precipitation from 1980 to 2010 (PPT_{AVG}), long-term mean temperature from 1980 to 2010 (TMP_{AVG}), and the slope of VPD during this period (VPD_{slp1}).

be related to the spatial coverage—our study area covers the entire California in which the spatial variations in precipitation is much higher. In addition, forests are generally located in higher elevation areas, and may have been buffered from the initial drought impact or even benefit from a higher temperature at the beginning of the drought (Figure 5c). Similarly, high elevation vegetation responded favorably to the 2003 heatwave in Europe, benefiting from an increasing temperature with adequate soil moisture (Jolly et al., 2005).

4. Conclusion

We use satellite records of vegetation greenness to study the biological patterns and environmental drivers of ecosystem response to an extreme and persistent drought—the 2012–2016 California Drought. By 2019, only 33% of the natural ecosystems recovered from the drought (i.e., areas with annual mean EVI higher than that of 2010), which has a significant implication on the carbon and water cycles. Most areas had abrupt changes caused by varying water availability, preceded by either positive or negative trends of productivity. We show three contrasting patterns of drought response that dominate the ecosystems of California: one with gradual decline in productivity, followed by an abrupt recovery, which was mainly driven by a temporary increase in precipitation (even when the annual precipitation was still below normal); the second one with a slow positive response before an abrupt decline in productivity which was due to a chronicle water deficit; and a third with both slow and abrupt decline in EVI. The spatiotemporal patterns of drought response are largely driven by environmental factors (e.g., long-term mean temperature and precipitation and/or temperature/precipitation during the drought) and biological factors (e.g., long-term average productivity).

Our results also suggest that ecosystem responses to drought can be complex, and the recovery process of the ecosystem is oftentimes non-linear. For high altitude forest ecosystems, initial benefits from the drought lasted longer than one growing season (unlike the 2012 US drought which had an increase in productivity in the spring, or 2003 Europe heatwave, which had an increase all year round). As temperature remained high while the water ran out (Goulden & Bales, 2019), forests lost 36% of the productivity gained during the initial stage of the drought. Areas with high productivity prior to drought could be more resistant. With the more frequent and more intense drought in this area (Cook et al., 2015), the resilience of the ecosystems will be tested, and this resistance will largely depend on a combination of biological factors (predrought productivity), precipitation, and temperature. In this area, forests may be more resilient than grasslands and shrublands in a short drought, but in the end, they may still succumb to future intense and prolonged drought.

Data Availability Statement

PRISM data can be downloaded https://prism.oregonstate.edu/. All source code can be downloaded from Zenodo (https://doi.org/10.5281/zenodo.4542105).

Acknowledgments
X. Yang is funded by the National Aeronautics and Space Administration (grant 80NSSC17K0110), National Science Foundation through Division of Integrative Organismal Systems (grant 2005574), and Center for Innovative Technology through Commonwealth Research Commercialization Fund. X. Xu acknowledges the funding from the Cornell College of Agriculture and Life Sciences. M. Chen is supported by a project of NASA Terrestrial Ecology Program: Arctic Boreal Vulnerability Experiment Phase 2, and a Laboratory Directed Research and Development project of the Pacific Northwest National Laboratory. MODIS data can be downloaded from NASA Earthdata (https://search.earthdata.nasa.gov/).

References

Adams, H. D., Zeppel, M. J. B., Anderegg, W. R. L., Hartmann, H., Landhäusser, S. M., Tissue, D. T., et al. (2017). A multi-species synthesis of physiological mechanisms in drought-induced tree mortality. *Nature Ecology & Evolution*, *1*(9), 1285–1291. https://doi.org/10.1038/s41559-017-0248-x

Allen, C. D., Breshears, D. D., & McDowell, N. G. (2015). On underestimation of global vulnerability to tree mortality and forest die-off from hotter drought in the Anthropocene. *Ecosphere*, *6*(8), 1–55. https://doi.org/10.1890/es15-00203.1

Anderegg, W. R. L., Flint, A., Huang, C.-Y., Flint, L., Berry, J. A., Davis, F. W., et al. (2015). Tree mortality predicted from drought-induced vascular damage. *Nature Geoscience*, *8*(5), 367–371. https://doi.org/10.1038/ngeo2400

Asner, G. P., Brodrick, P. G., & Anderson, C. B. (2016). *Progressive forest canopy water loss during the 2012–2015 California drought*. https://www.pnas.org/content/113/2/E249.short

Baldocchi, D. D., Xu, L., & Kiang, N. (2004). How plant functional-type, weather, seasonal drought, and soil physical properties alter water and energy fluxes of an oak-grass savanna and an annual grassland. *Agricultural and Forest Meteorology*. https://doi.org/10.1016/j.agrformet.2003.11.006

Berry, J., & Bjorkman, O. (1980). Photosynthetic response and adaptation to temperature in higher plants. *Annual Review of Plant Physiology*, *31*(1), 491–543. https://doi.org/10.1146/annurev.pp.31.060180.002423

Brodrick, P. G., & Asner, G. P. (2017). Remotely sensed predictors of conifer tree mortality during severe drought. *Environmental Research Letters*. https://doi.org/10.1088/1748-9326/aa8f55

Cook, B. I., Ault, T. R., & Smerdon, J. E. (2015). Unprecedented 21st century drought risk in the American Southwest and Central Plains. *Science Advances*, *1*(1), 1–8. https://doi.org/10.1126/sciadv.1400082

Daly, C., Taylor, G. H., & Gibson, W. P. (1997). The PRISM approach to mapping precipitation and temperature. In *Proceedings 10th AMS Conference on Applied Climatology* (pp. 20–23).

Demetillo, M. A. G., Anderson, J. F., Geddes, J. A., Yang, X., Najacht, E. Y., Herrera, S. A., et al. (2019). Observing severe drought influences on ozone air pollution in California. *Environmental Science and Technology*. https://doi.org/10.1021/acs.est.8b04852

Dietrich, L., Hoch, G., Kahmen, A., & Körner, C. (2018). Losing half the conductive area hardly impacts the water status of mature trees. *Scientific Reports*, *8*(1), 15006. https://doi.org/10.1038/s41598-018-33465-0

Diffenbaugh, N. S., Swain, D. L., Touma, D., & Lubchenco, J. (2015). Anthropogenic warming has increased drought risk in California. *Proceedings of the National Academy of Sciences of the United States of America*, *112*(13), 3931–3936. https://doi.org/10.1073/pnas.1422385112

Dong, C., MacDonald, G. M., Willis, K., Gillespie, T. W., Okin, G. S., & Williams, A. P. (2019). Vegetation responses to 2012-2016 drought in Northern and Southern California. *Geophysical Research Letters*, *46*(7), 3810–3821. https://doi.org/10.1029/2019gl082137

Dong, C., MacDonald, G., Okin, G. S., & Gillespie, T. W. (2019). Quantifying drought sensitivity of mediterranean climate vegetation to recent warming: A case study in Southern California. *Remote Sensing*, *11*(24), 2902. https://doi.org/10.3390/rs11242902

Famiglietti, J. S. (2014). The global groundwater crisis. *Nature Climate Change*, *4*(11), 945–948. https://doi.org/10.1038/nclimate2425

Fan, Y., Li, H., & Miguez-Macho, G. (2013). Global patterns of groundwater table depth. *Science*, *339*(6122), 940–943. https://doi.org/10.1126/science.1229881

Fettig, C. J., Mortenson, L. A., Bulaon, B. M., & Foulk, P. B. (2019). Tree mortality following drought in the central and southern Sierra Nevada, California, U.S. *Forest Ecology and Management*, *432*(2018), 164–178. https://doi.org/10.1016/j.foreco.2018.09.006

Flint, L. E., Flint, A. L., Thorne, J. H., & Boynton, R. (2013). Fine-scale hydrologic modeling for regional landscape applications: The California Basin Characterization Model development and performance. *Ecological Processes*, *2*(1), 1–21. https://doi.org/10.1186/2192-1709-2-25

Forkel, M., Carvalhais, N., Verbesselt, J., Mahecha, M., Neigh, C., & Reichstein, M. (2013). Trend change detection in NDVI time series: Effects of inter-annual variability and methodology. *Remote Sensing*, *5*(5), 2113–2144. https://doi.org/10.3390/rs5052113. https://doi.org/10.3390/rs5052113

Gaylord, M. L., Kolb, T. E., Pockman, W. T., Plaut, J. A., Yepez, E. A., Macalady, A. K., et al. (2013). Drought predisposes piñon-juniper woodlands to insect attacks and mortality. *New Phytologist*, *198*(2), 567–578. https://doi.org/10.1111/nph.12174

Goulden, M. L., & Bales, R. C. (2019). California forest die-off linked to multi-year deep soil drying in 2012–2015 drought. *Nature Geoscience*. https://doi.org/10.1038/s41561-019-0388-5

Griffin, D., & Anchukaitis, K. J. (2014). How unusual is the 2012-2014 California drought?. *Geophysical Research Letters*, *41*, 9017–9023. https://doi.org/10.1002/2014GL062433.1

Grossiord, C., Buckley, T. N., Cernusak, L. A., Novick, K. A., Poulter, B., Siegwolf, R. T. W., et al. (2020). Plant responses to rising vapor pressure deficit. *New Phytologist*, *226*(6), 1550–1566. https://doi.org/10.1111/nph.16485

Huang, M., Piao, S., Ciais, P., Peñuelas, J., Wang, X., Keenan, T. F., et al. (2019). Air temperature optima of vegetation productivity across global biomes. *Nature Ecology & Evolution*, *3*(5), 772–779. https://doi.org/10.1038/s41559-019-0838-x

Huete, A., Didan, K., Miura, T., Rodriguez, E. P., Gao, X., & Ferreira, L. G. (2002). Overview of the radiometric and biophysical performance of the MODIS vegetation indices. *Remote Sensing of Environment*, *83*(1–2), 195–213. https://doi.org/10.1016/S0034-4257(02)00096-2

Jolly, W. M., Dobbertin, M., Zimmermann, N. E., & Reichstein, M. (2005). Divergent vegetation growth responses to the 2003 heat wave in the Swiss Alps. *Geophysical Research Letters*, *32*(18), 1–4. https://doi.org/10.1029/2005GL023252

Kannenberg, S. A., Novick, K. A., Alexander, M. R., Maxwell, J. T., Moore, D. J. P., Phillips, R. P., & Anderegg, W. R. L. (2019). Linking drought legacy effects across scales: From leaves to tree rings to ecosystems. *Global Change Biology*, *25*(9), 2978–2992. https://doi.org/10.1111/gcb.14710

Körner, C. (2019). No need for pipes when the well is dry-a comment on hydraulic failure in trees. *Tree Physiology*, *39*(5), 695–700. https://doi.org/10.1093/treephys/tpz030

Malone, S. L., Tulbure, M. G., Pérez-Luque, A. J., Assal, T. J., Bremer, L. L., Drucker, D. P., et al. (2016). Drought resistance across California ecosystems: Evaluating changes in carbon dynamics using satellite imagery. *Ecosphere*, *7*(11), 1–19. https://doi.org/10.1002/ecs2.1561

McDowell, N. G., Allen, C. D., Anderson-Teixeira, K., Aukema, B. H., Bond-Lamberty, B., Chini, L., et al. (2020). Pervasive shifts in forest dynamics in a changing world. *Science*, *368*(6494). https://doi.org/10.1126/science.aaz9463

McDowell, N. G., Michaletz, S. T., Bennett, K. E., Solander, K. C., Xu, C., Maxwell, R. M., & Middleton, R. S. (2018). Predicting chronic climate-driven disturbances and their mitigation. *Trends in Ecology & Evolution*, *33*(1), 15–27. https://doi.org/10.1016/j.tree.2017.10.002

McDowell, N., Pockman, W. T., Allen, C. D., Breshears, D. D., Cobb, N., Kolb, T., et al. (2008). Mechanisms of plant survival and mortality during drought: why do some plants survive while others succumb to drought?. *New Phytologist*, *178*(4), 719–739. https://doi.org/10.1111/j.1469-8137.2008.02436.x

Miller, D. L., Alonzo, M., Roberts, D. A., Tague, C. L., & McFadden, J. P. (2020). Drought response of urban trees and turfgrass using airborne imaging spectroscopy. *Remote Sensing of Environment*, *240*, 111646. https://doi.org/10.1016/j.rse.2020.111646

Muggeo, V. M. R., & Others (2008). Segmented: An R package to fit regression models with broken-line relationships. *R News*, *8*(1), 20–25. ftp://rm.mirror.garr.it/mirrors/CRAN/doc/Rnews/Rnews_2008-1-1.pdf#page=20

Paz-Kagan, T., Brodrick, P. G., Vaughn, N. R., Das, A. J., Stephenson, N. L., Nydick, K. R., & Asner, G. P. (2017). What mediates tree mortality during drought in the southern Sierra Nevada?. *Ecological Applications*, *27*(8), 2443–2457. https://doi.org/10.1002/eap.1620

Rao, K., Anderegg, W. R. L., Sala, A., Martínez-Vilalta, J., & Konings, A. G. (2019). Satellite-based vegetation optical depth as an indicator of drought-driven tree mortality. *Remote Sensing of Environment*, *227*, 125–136. https://doi.org/10.1016/j.rse.2019.03.026

Reichstein, M., Bahn, M., Ciais, P., Frank, D., Mahecha, M. D., Seneviratne, S. I., et al. (2013). Climate extremes and the carbon cycle. *Nature*, *500*(7462), 287–295. https://doi.org/10.1038/nature12350

Scheff, J., & Frierson, D. M. W. (2012). Robust future precipitation declines in CMIP5 largely reflect the poleward expansion of model subtropical dry zones. *Geophysical Research Letters*, *39*(17), 1–6. https://doi.org/10.1029/2012GL052910

Scholes, R. J., & Archer, S. R. (1997). Tree-grass interactions in Savannas. In *Annual Review of Ecology and Systematics*. https://doi.org/10.1146/annurev.ecolsys.28.1.517

Schwalm, C. R., Anderegg, W. R. L., Michalak, A. M., Fisher, J. B., Biondi, F., Koch, G., et al. (2017). Global patterns of drought recovery. *Nature*, *548*(7666), 202–205. https://doi.org/10.1038/nature23021

Sperry, J. S., Venturas, M. D., Anderegg, W. R. L., Mencuccini, M., Mackay, D. S., Wang, Y., & Love, D. M. (2017). Predicting stomatal responses to the environment from the optimization of photosynthetic gain and hydraulic cost. *Plant, Cell and Environment*, *40*(6), 816–830. https://doi.org/10.1111/pce.12852

Stovall, A. E. L., Shugart, H. H., & Yang, X. (2019). Tree height explains mortality risk during an intense drought. *Nature Communications*, *10*(2019), 4385. https://doi.org/10.1038/s41467-019-12380-6

Stovall, A. E. L., Shugart, H. H., & Yang, X. (2020). Reply to "Height-related changes in forest composition explain increasing tree mortality with height during an extreme drought. *Nature Communications*, *11*(1), 3401. https://doi.org/10.1038/s41467-020-17214-4

Trugman, A. T., Detto, M., Bartlett, M. K., Medvigy, D., Anderegg, W. R. L., Schwalm, C., et al. (2018). Tree carbon allocation explains forest drought-kill and recovery patterns. *Ecology Letters*, *21*(10), 1552–1560. https://doi.org/10.1111/ele.13136

Verbesselt, J., Hyndman, R., Zeileis, A., & Culvenor, D. (2010). Phenological change detection while accounting for abrupt and gradual trends in satellite image time series. *Remote Sensing of Environment*, *114*(12), 2970–2980. https://doi.org/10.1016/j.rse.2010.08.003

Vicente-Serrano, S. M., Gouveia, C., Camarero, J. J., Beguería, S., Trigo, R., López-Moreno, J. I., et al. (2013). Response of vegetation to drought time-scales across global land biomes. *Proceedings of the National Academy of Sciences*, *110*(1), 52–57. https://doi.org/10.1073/pnas.1207068110

Williams, A. P., Seager, R., Abatzoglou, J. T., Cook, B. I., Smerdon, J. E., & Cook, E. R. (2015). Contribution of anthropogenic warming to California drought during 2012-2014. *Geophysical Research Letters*, *42*, 6819–6828. https://doi.org/10.1002/2015gl064924

Wolf, S., Keenan, T. F., Fisher, J. B., Baldocchi, D. D., Desai, A. R., Richardson, A. D., et al. (2016). Warm spring reduced carbon cycle impact of the 2012 US summer drought. *Proceedings of the National Academy of Sciences of the United States of America*, *113*(21), 5880–5885. https://doi.org/10.1073/pnas.1519620113

Xu, X., Medvigy, D., & Rodriguez-Iturbe, I. (2015). Relation between rainfall intensity and savanna tree abundance explained by water use strategies. *Proceedings of the National Academy of Sciences of the United States of America*, *112*(42), 12992–12996. https://doi.org/10.1073/pnas.1517382112

Young, D. J. N., Stevens, J. T., Earles, J. M., Moore, J., Ellis, A., Jirka, A. L., & Latimer, A. M. (2017). Long-term climate and competition explain forest mortality patterns under extreme drought. *Ecology Letters*, *20*(1), 78–86. https://doi.org/10.1111/ele.12711

Zhao, K., Wulder, M. A., Hu, T., Bright, R., Wu, Q., Qin, H., et al. (2019). Detecting change-point, trend, and seasonality in satellite time series data to track abrupt changes and nonlinear dynamics: A Bayesian ensemble algorithm. *Remote Sensing of Environment*, *232*, 111181. https://doi.org/10.1016/j.rse.2019.04.034